Supporting Information

TiO_2 nanocolumn arrays for more efficient and stable perovskite solar cells

Zhelu Hu,[a] José Miguel García-Martín,[b] Yajuan Li,[c] Laurent Billot,[a] Baoquan Sun,[c] Fernando Fresno,[d] Antonio García-Martín,[b] María Ujué González,[b] Lionel Aigouy,[a] Zhuoying Chen[*a]*

a. LPEM, ESPCI Paris, PSL Research University, Sorbonne Université, CNRS, 10 Rue Vauquelin, F-75005 Paris, France

b. Instituto de Micro y Nanotecnología IMN-CNM, CSIC, CEI UAM+CSIC, Isaac Newton 8, E-28760 Tres Cantos, Madrid, Spain

c. Jiangsu Key Laboratory for Carbon-Based Functional Materials & Devices, Institute of Functional Nano & Soft Materials (FUNSOM), Soochow University, 199 Ren'ai Road, Suzhou, 215123, Jiangsu, PR China

d. Photoactivated Processes Unit, IMDEA Energy Institute, Avda. Ramón de la Sagra, 3, 28935 Móstoles, Madrid, Spain.

* Corresponding author. E-mail: zhuoying.chen@espci.fr

I. Morphology characterizations on the surface of compact-TiO_2 (cp-TiO_2) and bare FTO before and after the nanocolumn fabrication procedure and thermal treatment.

As the control samples also underwent the thermal treatment, AFM imaging was performed before and after the process onto the FTO and the continuous cp-TiO_2 layers. A substrate corner was intentionally left un-covered by cp-TiO_2 exposing the bare FTO underneath. As it can be seen in the Figure S1 for FTO and in the Figure S2 for the planar cp-TiO_2 below, neither the morphology nor the roughness of the layers changed.

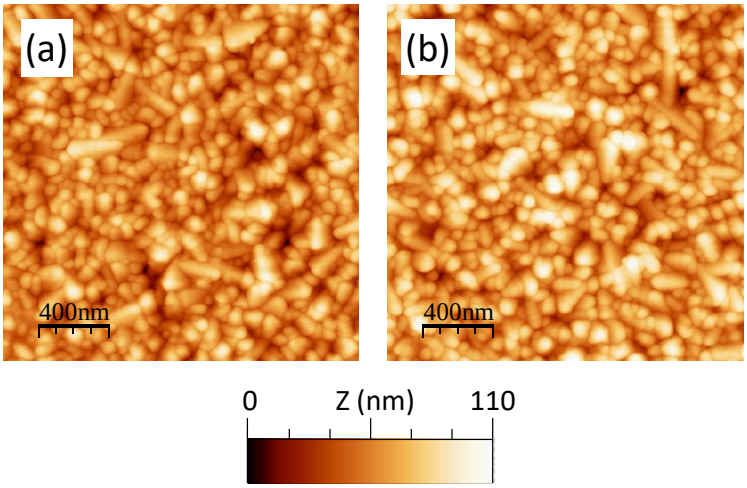

Figure S1: Representative AFM images of a bare FTO before (a) and after (b) the thermal treatment.

The average root mean square (rms) roughness for FTO was 15 nm initially and 15.6 nm after the oxidation, whereas for cp-TiO_2 was 9.5 nm before and 9.4 nm after the treatment.

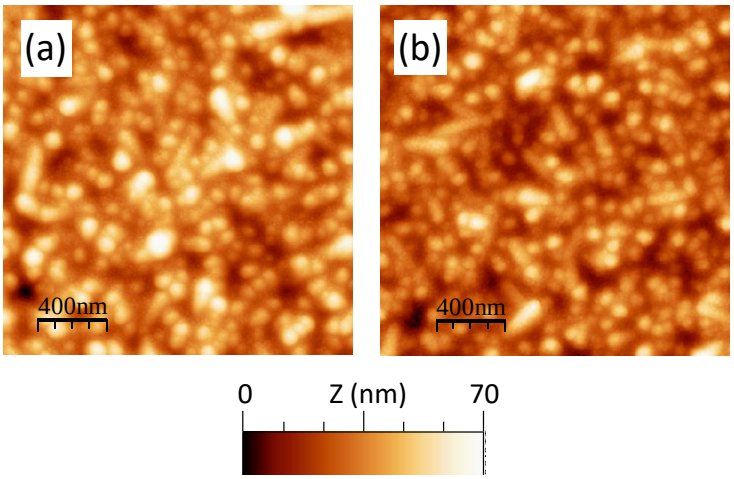

Figure S2: Representative AFM images of cp-TiO_2 before (a) and after (b) the thermal treatment.

II. AFM characterizations of the perovskite layer deposited on cp-TiO_2 and TiO_2 nanocolumns

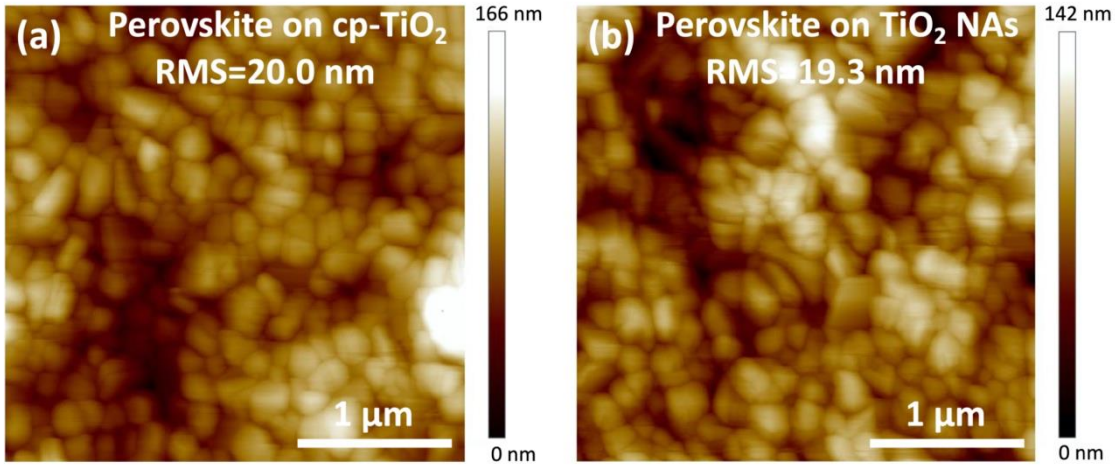

Figure S3: Representative AFM images of the perovskite layer deposited on the cp-TiO_2 (a) and on TiO_2 nanocolumns (b).

III. Optical absorbance spectra of perovskite films deposited onto TiO_2 nanocolumns and cp-TiO_2

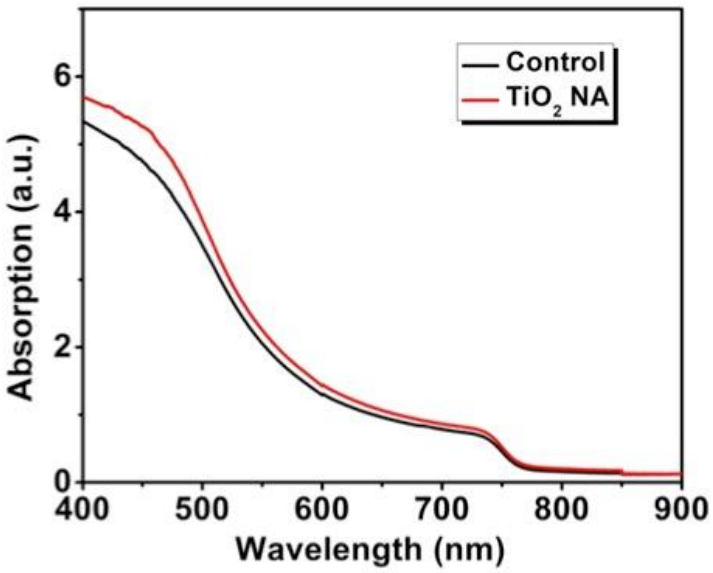

Figure S4: The optical absorbance spectra of the perovskite film deposited on a cp-TiO_2/FTO glass substrate (control sample) and on a TiO_2 NA/cp-TiO_2/FTO glass substrate, respectively.

IV. UV degradation behaviors of perovskite solar cells built on TiO_2 nanocolumns and on cp-TiO_2 ETL

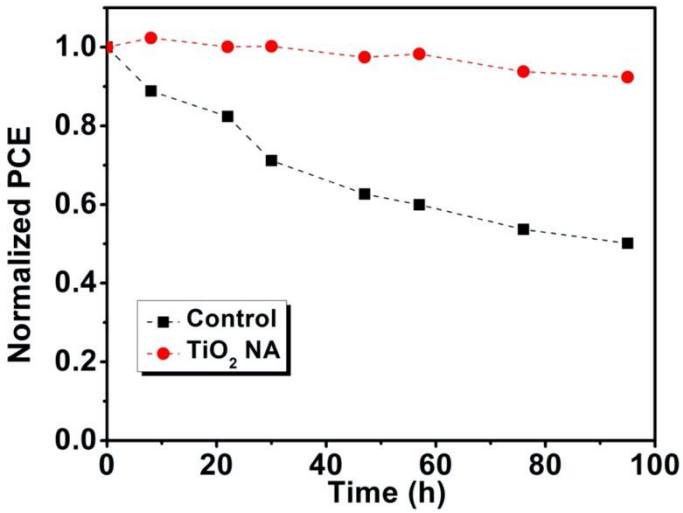

Figure S5: The evolution of the power conversion efficiency (PCE) under constant UV illumination (λ = 365 nm, 3 mW cm^{-2}) in argon atmosphere measured on the perovskite solar cells built on the cp-TiO_2 ETL (control condition) and on TiO_2 nanocolumns arrays of the same substrate.

V. XRD and SEM characterizations of TiO_2 nanocolumns from Ti nanocolumn arrays by thermal oxidation

The second step of the preparation of TiO_2 nanocolumn arrays, i.e. the thermal oxidation of the Ti nanocolumn arrays to obtain TiO_2 nanocolumns, has been characterized by means of AFM, SEM and XRD.

The transformation of the metal into oxide was monitored by XRD. X-ray diffractograms of the initial metallic Ti nanocolums and the TiO_2 nanocolumns obtained after oxidation are shown in Figure S3. Initially, only reflections corresponding to metallic titanium are visible, which after the thermal oxidation procedure have completely disappeared. In turn, the reflections observed after treatment show the oxidized nanocolumns to be formed by the rutile phase of TiO_2. A small contribution of the anatase phase of TiO_2 is suggested as well by the shoulder appearing at 2θ ca. 25.4°.

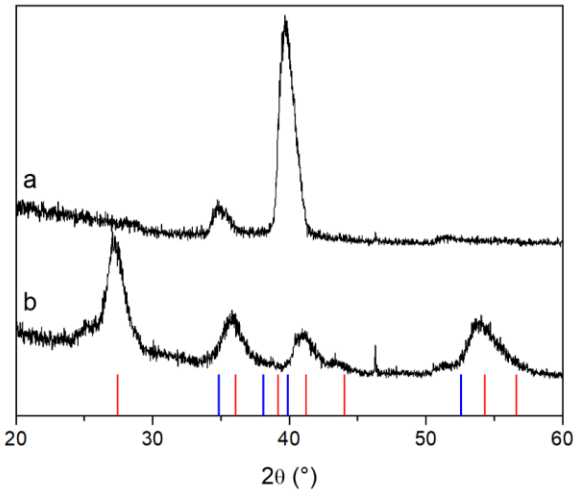

Figure S6: X-ray diffractograms of the nanocolumn arrays before (a) and after (b) the thermal oxidation treatment. Bars correspond to the reflections of Ti metal (blue, ICDD PDF # 01-071-4632) and rutile TiO_2 (red, ICDD PDF # 01-072-1148).

The process induced morphological and structural changes on the nanocolumns array. Figure S7 shows SEM images of the initial Ti nanocolumns and of the resulting TiO_2 ones. A broadening of the nanocolumns was observed, as it could be expected from the incorporation of a large amount of oxygen. Such broadening even produces the coalescence of neighboring nanocolumns that were initially too close, as it can be seen in Figure S7(b). However, the 1D nanocolumn nature of the sample was kept.

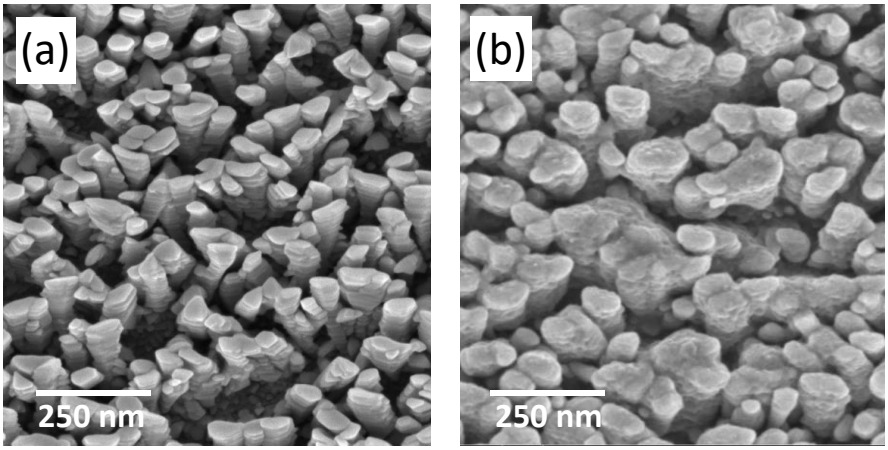

Figure S7: Representative SEM images of as-deposited Ti nanocolumns (a) and of the resulting TiO_2 nanocolumns after the thermal treatment (b).

Table S1. Photovoltaic parameters with standard distribution of the perovskite solar cells built onto different substrates. Each substrate contains half of it covered by cp-TiO_2 ETL another half covered by TiO_2 nanocolumn arrays. Each error bar was obtained from eight solar cells fabricated and measured by the same conditions.

ETL	J_{sc} (mA/cm^2)	V_{oc} (V)	*FF* (%)	*PCE* (%)
cp-TiO_2	19.43 ± 0.22	1.06 ± 0.02	72.90 ± 0.86	14.96 ± 0.28
TiO_2 NA	20.13 ± 0.21	1.07 ± 0.02	74.41 ± 1.27	15.97 ± 0.33

Table S2. EIS parameters for the perovskite solar cells with TiO_2 nanocolumn (NA) ETL and cp-TiO_2 ETL.

ETL	R_s (Ω)	R_{tr} (Ω)	R_{rec} (Ω)	CPE_{ct}-T (F)	CPE_{ct}-P	CPE_{rec}-T (F)	CPE_{rec}-P
cp-TiO_2	10.05	20.02	2085	2.71×10^{-9}	1.08	1.44×10^{-8}	0.97
TiO_2 NA	10.08	13.52	4410	1.85×10^{-8}	1.35	8.08×10^{-7}	1.00